NAVAL POSTGRADUATE SCHOOL
Monterey, California

THESIS

SEMI-RIGID TOWING MODEL FOR ANALYSIS OF MANEUVERING IN THE HORIZONTAL PLANE

by

Garrett D. Jones

September 2001

Thesis Advisor: Fotis A. Papoulias

Approved for public release; distribution is unlimited.

Report Documentation Page

Report Date	Report Type	Dates Covered (from... to)
30 Sep 2001	N/A	-

Title and Subtitle Semi-rigid Towing Model For Analysis of Maneuvering in The Horizontal Plane	**Contract Number**
	Grant Number
	Program Element Number
Author(s) Jones, Garrett D.	**Project Number**
	Task Number
	Work Unit Number
Performing Organization Name(s) and Address(es) Research Office Naval Postgraduate School Monterey, Ca 93943-5138	**Performing Organization Report Number**
Sponsoring/Monitoring Agency Name(s) and Address(es)	**Sponsor/Monitor's Acronym(s)**
	Sponsor/Monitor's Report Number(s)
Distribution/Availability Statement Approved for public release, distribution unlimited	
Supplementary Notes	
Abstract	
Subject Terms	
Report Classification unclassified	**Classification of this page** unclassified
Classification of Abstract unclassified	**Limitation of Abstract** UU
Number of Pages 62	

REPORT DOCUMENTATION PAGE			Form Approved OMB No. 0704-0188
Public reporting burden for this collection of information is estimated to average 1 hour per response, including the time for reviewing instruction, searching existing data sources, gathering and maintaining the data needed, and completing and reviewing the collection of information. Send comments regarding this burden estimate or any other aspect of this collection of information, including suggestions for reducing this burden, to Washington headquarters Services, Directorate for Information Operations and Reports, 1215 Jefferson Davis Highway, Suite 1204, Arlington, VA 22202-4302, and to the Office of Management and Budget, Paperwork Reduction Project (0704-0188) Washington DC 20503.			
1. AGENCY USE ONLY *(Leave blank)*	**2. REPORT DATE** September 2001	**3. REPORT TYPE AND DATES COVERED** Master's Thesis	
4. TITLE AND SUBTITLE: Semi-rigid Towing Model For Analysis of Maneuvering in The Horizontal Plane			**5. FUNDING NUMBERS**
6. AUTHOR(S) Jones, Garrett D.			
7. PERFORMING ORGANIZATION NAME(S) AND ADDRESS(ES) Naval Postgraduate School Monterey, CA 93943-5000			**8. PERFORMING ORGANIZATION REPORT NUMBER**
9. SPONSORING / MONITORING AGENCY NAME(S) AND ADDRESS(ES) N/A			**10. SPONSORING / MONITORING AGENCY REPORT NUMBER**
11. SUPPLEMENTARY NOTES The views expressed in this thesis are those of the author and do not reflect the official policy or position of the Department of Defense or the U.S. Government.			
12a. DISTRIBUTION / AVAILABILITY STATEMENT Approved for public release; distribution is unlimited.			**12b. DISTRIBUTION CODE**

13. ABSTRACT ***(maximum 200 words)***

A SIMULINK towing model is developed from the surge, sway, and yaw equations of motion in order to study the horizontal maneuverability of vessels in a semi-rigid towing operation. This analysis is conducted in order to validate rigid-connection towing and to give insight into the design of the tow connector. The connection is modeled as a linear spring and the maneuverability of the vessels is studied as the stiffness is varied from conditions of semi to completely rigid. This study is based on two Swath hull vessels, the SLICE and KAIMALINO, towing in close proximity under calm water conditions.

14. SUBJECT TERMS CLOSE-PROXIMITY TOWING, DIRECTIONAL STABILITY, SIMULATION MODEL, SIMULINK			**15. NUMBER OF PAGES** 49
			16. PRICE CODE
17. SECURITY CLASSIFICATION OF REPORT Unclassified	**18. SECURITY CLASSIFICATION OF THIS PAGE** Unclassified	**19. SECURITY CLASSIFICATION OF ABSTRACT** Unclassified	**20. LIMITATION OF ABSTRACT** UL

NSN 7540-01-280-5500

Standard Form 298 (Rev. 2-89)
Prescribed by ANSI Std. 239-18

THIS PAGE INTENTIONALLY LEFT BLANK

Approved for public release; distribution is unlimited.

SEMI-RIGID TOWING MODEL FOR ANALYSIS OF MANUEVERING IN THE HORIZONTAL PLANE

Garrett D. Jones
Lieutenant, United States Navy
B.A., United States Naval Academy, 1994

Submitted in partial fulfillment of the
requirements for the degree of

MASTER OF ARTS OR SCIENCE IN MECHANICAL ENGINEERING

from the

NAVAL POSTGRADUATE SCHOOL
September, 2001

Author: _____
Garrett D. Jones

Approved by: _____
Fotis A. Papoulias, Thesis Advisor

_____
Terry McNelley, Chairman
Department or Mechanical Engineering

THIS PAGE INTENTIONALLY LEFT BLANK

ABSTRACT

A SIMULINK towing model is developed from the surge, sway, and yaw equations of motion in order to study the horizontal maneuverability of vessels in a semi-rigid towing operation. This analysis is conducted in order to validate rigid-connection towing and to give insight into the design of the tow connector. The connection is modeled as a linear spring and the maneuverability of the vessels is studied as the stiffness is varied from conditions of semi to completely rigid. This study is based on two Swath hull vessels, the SLICE and KAIMALINO, towing in close proximity under calm water conditions.

THIS PAGE INTENTIONALLY LEFT BLANK

TABLE OF CONTENTS

THIS PAGE INTENTIONALLY LEFT BLANK

LIST OF FIGURES

THIS PAGE INTENTIONALLY LEFT BLANK

LIST OF TABLES

THIS PAGE INTENTIONALLY LEFT BLANK

I. INTRODUCTION

As part of a continuing program to advance in the swath hull technology, this paper looks into the feasibility of towing operation between the Slice and Kaimalino. The Slice is an advanced high-speed vessel that is emerging as a ship with a very wide range of open ocean capabilities. The Office of Naval Research desires to further showcase the advantage of multi-hull design by demonstrating the maneuverability of the Slice and Kaimalino during towing operations. Although numerous investigations have been conducted on optimizing towing connection points, towline length, and tension of towline, this study will be concerned with close proximity towing under a near rigid tow connector. Furthermore, most previous studies model the dynamics of the trailing ship only while the leading ship is treated as a point mass. This thesis models the coupled maneuvering motions of the two vessels.

A. KAIMALINO

The SSP Kaimalino was the world's first high performance open ocean Swath ship. It consists of two parallel torpedo-like hulls. Attached to the hulls are two streamlined struts. The struts extend above the water surface and support the main body. The Kaimalino also has stabilizing fins attached near the aft end of each hull. Figure 1 shows a profile of the SSP Kaimalino. The performance features of the Kaimalino are greatly reduced motions with sustained speed even in high sea states, lower hydrodynamic drag and reduced power requirements at moderate to high speeds, and excellent course keeping characteristics at all sea headings.

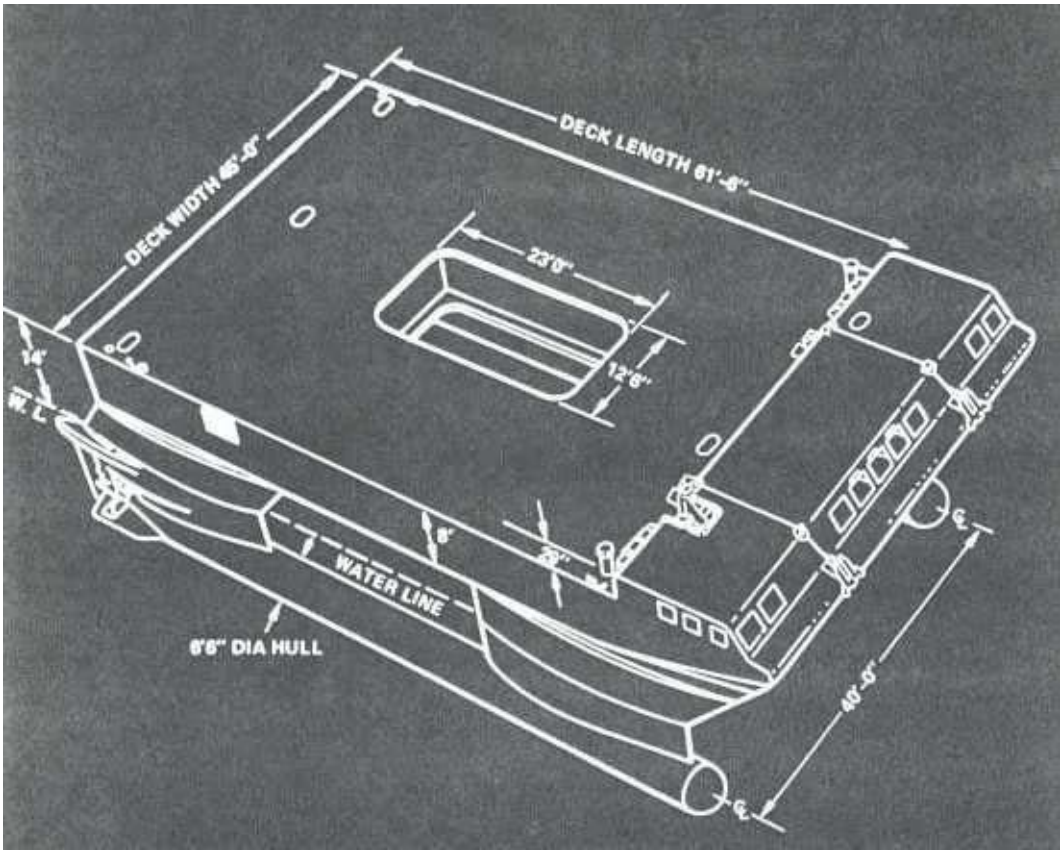

Figure 1. SSP KAIMALINO General Arrangements from Reference [8].

Length	88.6 ft
Beam	45.9 ft
Height	31.8 ft
Displacement	217 tons
Payload	50 tons
Max Speed	25 kt
Operational Speed	13 kt
Range	400 n miles

Table 1. KAIMALINO characteristics.

B. SLICE

The Slice is a high speed variant of the Swath technology. It has 4 underwater hulls instead of two. Attached to each hull is a strut that extends up to support the main body. Figure 2 and 3 show the profile view and the stern view of the Slice respectively. The Slice produces higher speeds for constant horsepower when compared to conventional Swath hulls and still maintains the good sea-keeping of Swath technology. The key innovation is reduction of wavemaking drag accomplished by using short struts, submerged hulls, and speeds well beyond the critical "hump" on the Froude resistance curve [1].

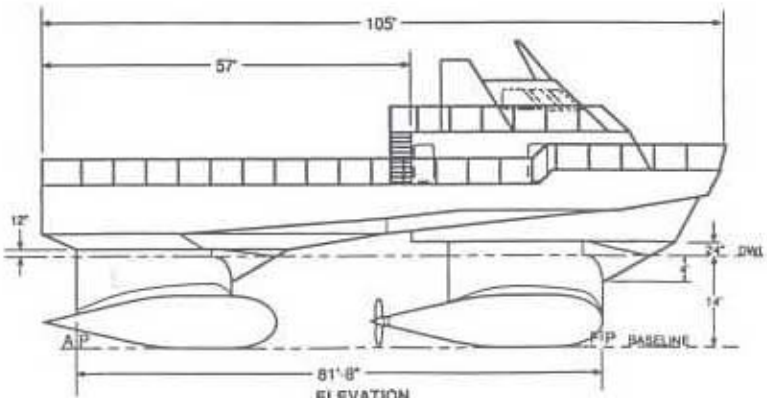

Figure 2. Profile view of SLICE vessel from Reference [10].

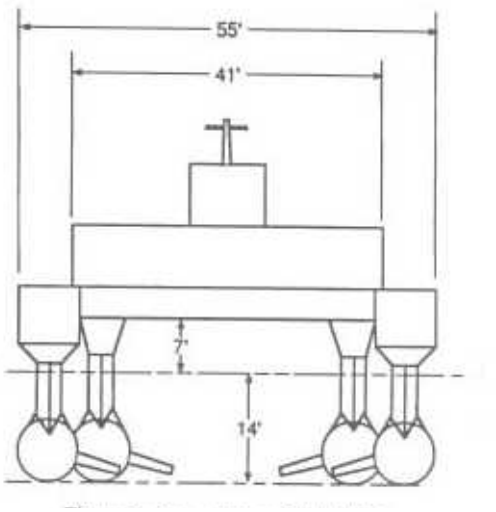

Figure 3. Stern view of SLICE vessel from Reference [10].

Length overall	105 ft
Beam	55 ft
Draft	14.1 ft
Displacement	180 tons
Max Speed	30 kt
Operational Speed	27 kt
Range	450 n miles

Table 2. SLICE characteristics.

THIS PAGE INTENTIONALLY LEFT BLANK

II. MANUEVERING ANALYSIS

A. EQUATIONS OF MOTION IN THE HORIZONTAL PLANE

For the case of horizontal plane maneuvering, the vertical plane motions are ignored, leaving only the surge, sway and yaw equations of motions (EOM) for the equation set. These equations will be developed with the assumptions that x_G and y_G are zero, and vehicle symmetry for its inertial properties. Also in the derivation of the EOM, two sets of axes are used, the inertial frame and the body fixed frame. The inertial frame is relative to the earth, ignoring the earth's rotational rate versus the vessel's rotational rate. Newton's Law is applied in the inertial reference frame. The body fixed frame is relative to the ship's center of gravity having the positive x-axis forward of the ship, starboard for positive y-axis, and down for positive z-axis. Applying Newton's law in the inertial reference frame results in the following equations for surge, sway, and yaw,

$$m\ddot{x}_0 = X_0 \tag{1}$$

$$m\ddot{y}_0 = Y_0 \tag{2}$$

$$I_Z\ddot{\psi} = N \tag{3}$$

where X_0 and Y_0 are the total forces in respective directions and N is the turning moment about the z-axis. Detailed in Reference [4] are the components that usually make up the total forces and moments. These total forces are a combination of fluid forces acting on the main body, control surface forces (i.e. rudders, fins, bow planes), environmental forces, and propulsion forces. Looking at the diagram below, it is easily shown that a relationship can be developed for transformation from inertial reference frame to the body fixed frame.

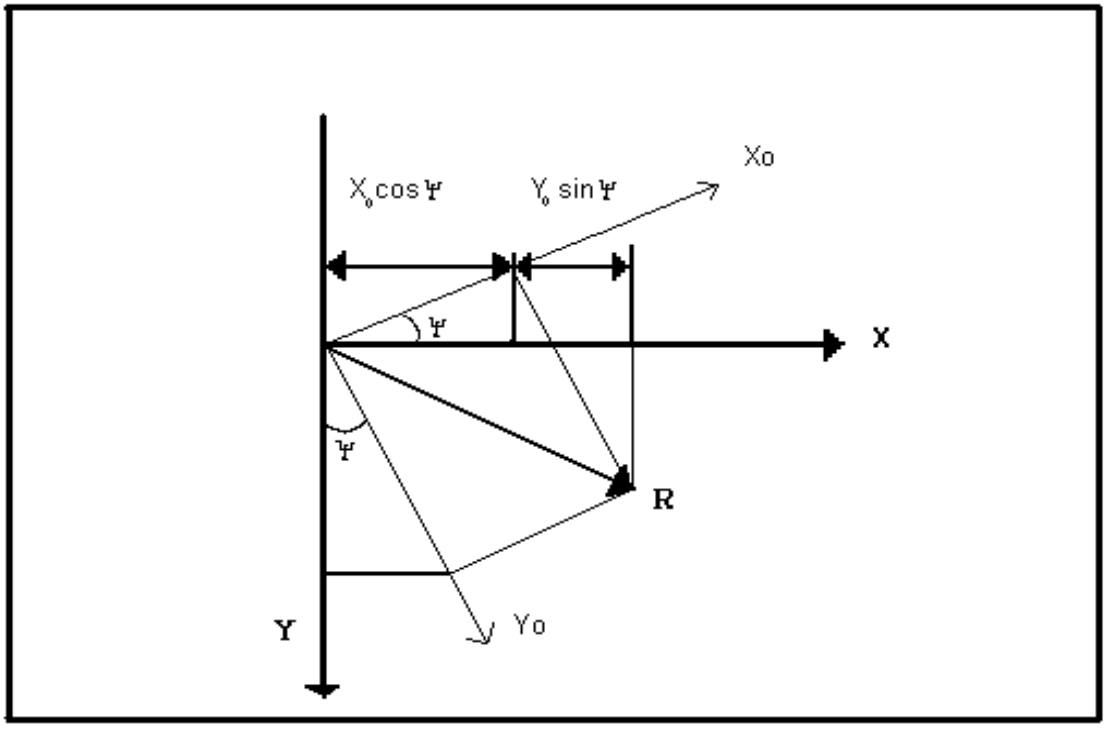

Figure 4. Relationship of position between two reference frames.

Therefore we transform coordinate systems using

$$X = X_0 \cos\psi + Y_0 \sin\psi \tag{4}$$

$$Y = Y_0 \cos\psi - X_0 \sin\psi \tag{5}$$

and for similar velocity diagrams

$$\dot{x} = u\cos\psi - v\sin\psi \tag{6}$$

$$\dot{y} = u\sin\psi + v\cos\psi \tag{7}$$

The rate of yaw is given by $\dot{\psi}$=r. Then differentiating the above equations with respect to time results in

$$\ddot{x} = \dot{u}\cos\psi - u\dot{\psi}\sin\psi - \dot{v}\sin\psi - v\dot{\psi}\cos\psi \tag{8}$$

$$\ddot{y} = \dot{u}\cos\psi - u\dot{\psi}\sin\psi - \dot{v}\sin\psi - v\dot{\psi}\cos\psi \tag{9}$$

Substituting these results into Equation (1) through (3) then into Equations (4) and (5) results in the following,

$$m\dot{u} - mvr = X \tag{10}$$

$$m\dot{v} + mur = Y \tag{11}$$

$$I_Z\dot{r} = N \tag{12}$$

where the u is the surge velocity, v is the sway velocity and r is the yaw velocity.

Now expressions for the right hand side (the forces) need to be developed. The environmental forces will be neglected for this study and the propulsion force will be designated only as X_{prop}. Neglecting any side propulsion forces resulting from torque, the total propulsion force acts only in the longitudinal direction for the surface vessel. For the fluid and rudder forces, the nonlinear components are complicated and expressions to approximate those components are still in development. The fluid forces will be linearized using a Taylor series expansion of forces as steady state functions in order to produce body forces represented as hydrodynamic coefficients. The hydrodynamic forces are functions of vessel velocities and accelerations. Expressions will be developed for small deviations from a nominal condition of straight line transit at a constant speed U.

$$\begin{aligned} Y_F = (Y_F)_0 + \frac{\partial Y_F}{\partial u}(u-u_0) + \frac{\partial Y_F}{\partial v}(v-v_0) + \frac{\partial Y_F}{\partial r}(r-r_0) + \frac{\partial Y_F}{\partial \dot{u}}(\dot{u}-\dot{u}_0) + \\ \frac{\partial Y_F}{\partial \dot{v}}(\dot{v}-\dot{v}_0) + \frac{\partial Y_F}{\partial \dot{r}}(\dot{r}-\dot{r}_0) \end{aligned} \tag{13}$$

where the subscript F is used for fluid force.

For the nominal condition stated above, the initial conditions are as follows.

$$u_0 = U$$
$$v_0 = \dot{u}_0 = \dot{v}_0 = r_0 = \dot{r}_0 = 0$$

Since the ship is acting in straight line motion there is no initial transverse force. Also because of symmetry, changes in the longitudinal velocity and acceleration produce no transverse force, $\partial Y/\partial u$ and $\partial Y/\partial \dot{u}$ are zero.

$$Y_F = \frac{\partial Y_F}{\partial v}(v) + \frac{\partial Y_F}{\partial r}(r) + \frac{\partial Y_F}{\partial \dot{v}}(\dot{v}) + \frac{\partial Y_F}{\partial \dot{r}}(\dot{r}) \tag{14}$$

Similar logic leads to the resulting expressions for surge and yaw.

$$X_F = \frac{\partial X_F}{\partial u}(u - U) + \frac{\partial X_F}{\partial \dot{u}} \tag{15}$$

$$N_F = \frac{\partial N_F}{\partial v}v + \frac{\partial N_F}{\partial \dot{v}}\dot{v} + \frac{\partial N_F}{\partial r}r + \frac{\partial N_F}{\partial \dot{r}}\dot{r} \tag{16}$$

The following notation for the derivatives will be used for the remainder of this paper; $\partial X/\partial u$ is X_u, $\partial Y/\partial u$ is Y_u, $\partial X/\partial \dot{u}$ is $X_{\dot{u}}$ etc… These are the hydrodynamic derivatives.

Assuming that the rudder forces and moments on the ship are functions of delta only, they too can be linearized. The rudder deflection angle is represented by δ. A positive δ means vessel is turning to port and negative δ is for turn to starboard. Expressions for the rudder forces and moments are presented below.

$$X_R = X_R(\delta = 0) + \frac{\partial X_R}{\partial \delta}\delta = 0 \tag{17}$$

$$Y_R = Y_R(\delta = 0) + \frac{\partial Y_R}{\partial \delta}\delta = Y_\delta \delta \tag{18}$$

$$N_R = N_R(\delta = 0) + \frac{\partial N_R}{\partial \delta}\delta = N_\delta \delta \tag{19}$$

The subscript R is used for rudder forces.

Substituting back into equations (10) through (12), we get the following EOMs for surge, sway and yaw.

$$(m - X_{\dot{u}})\dot{u} = X_u(u - U) + X_{prop} + X_\delta \delta \tag{20}$$

$$(m - Y_{\dot{v}})\dot{v} - Y_{\dot{r}}\dot{r} = Y_v v + (Y_r - mU)r + Y_\delta \delta \tag{21}$$

$$(I_Z - N_{\dot{r}})\dot{r} - N_{\dot{v}}\dot{v} = N_v v + N_r r + N_\delta \delta \tag{22}$$

B. EQUATIONS OF MOTION FOR THE SLICE AND KAIMALINO

In developing the EOMs for the towing model, another force had to be added. This force results from the tension in the towing connection. Using only the forces in the horizontal plane, this force is expressed as some variable spring constant K times the difference between the SLICE and Kaimalino positions. The towing operation to be modeled is shown in Figure 5.

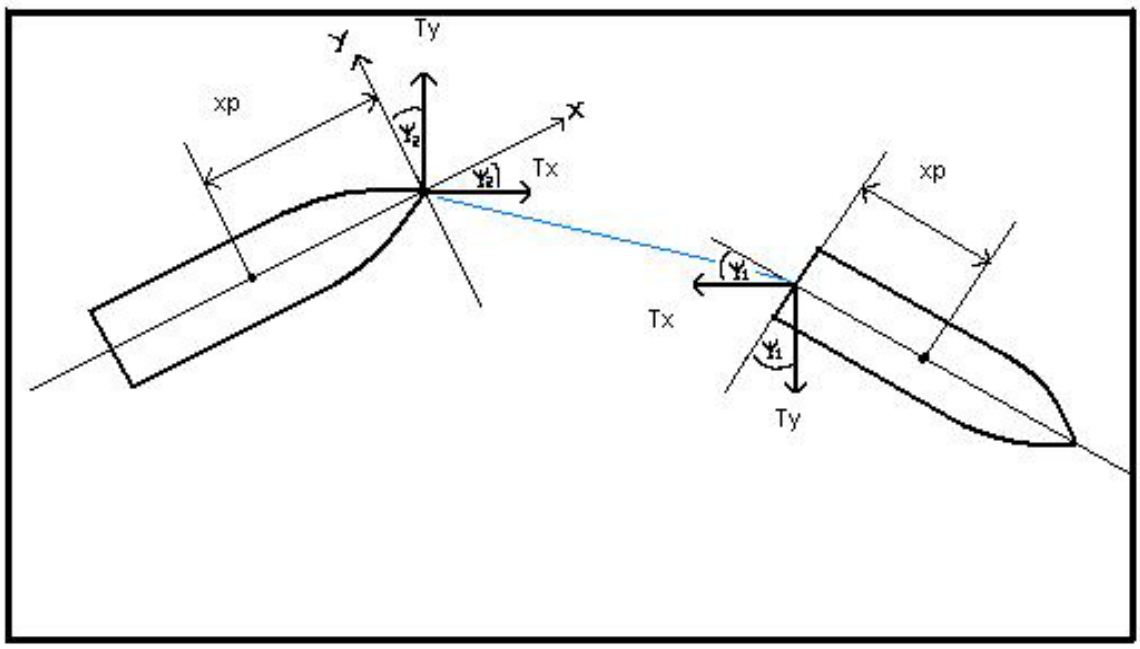

Figure 5. Diagram of tension forces resulting from vessels under tow.

$$T_x = k_x(x_{c,1} - x_{c,2}) \tag{23}$$

$$T_y = k_y(y_{c,1} - y_{c,2}) \tag{24}$$

subscript 1 represents the SLICE and subscript 2 is for the Kaimalino. This linear relationship expressing the tension forces couples the SLICE and Kaimalino EOMs. K_y and K_x are taking at various values in order to analyze the maneuverability of the vessels in towing operation. Below are the complete EOMs for the SLICE and Kaimalino.

$$(m_1 - X_{\dot{u}1})\dot{u}_1 - m_1 r_1 v_1 = -R_1 + X_{prop} - T_x \cos\psi_1 + T_y \sin\psi_1 \tag{25}$$

$$(m_1 - Y_{\dot{v}1})\dot{v}_1 - Y_{\dot{r}1}\dot{r}_1 + m_1 r_1 u_1 = Y_{v1} v_1 + Y_{r1} r_1 - T_y \cos\psi_1 - T_x \sin\psi_1 + Y_\delta \delta \tag{26}$$

$$(I_{Z1} - N_{\dot{r}1})\dot{r}_1 - N_{\dot{v}1}\dot{v}_1 = N_{v1} v_1 + N_{r1} r_1 + x_{p1}(T_x \sin\psi_1 + T_y \cos\psi_1) + N_\delta \delta \tag{27}$$

$$(m_2 - X_{\dot{u}2})\dot{u}_2 - m_2 r_2 v_2 = -R_2 + T_x \cos\psi_2 + T_y \sin\psi_2 \tag{28}$$

$$(m_2 - Y_{\dot{v}2})\dot{v}_2 - Y_{\dot{r}2}\dot{r}_2 + m_2 r_2 u_2 = Y_{v2} v_2 + Y_{r2} r_2 + T_y \cos\psi_2 - T_x \sin\psi_2 \tag{29}$$

$$(I_{Z2} - N_{\dot{r}2})\dot{r}_2 - N_{\dot{v}2}\dot{v}_2 = N_{v2} v_2 + N_{r2} r_2 + x_{p2}(T_y \cos\psi_2 - T_x \sin\psi_2) \tag{30}$$

where ψ_1 and ψ_2 are the yaw angles of the SLICE and Kaimalino respectively. R_1 and R_2, the resistance of the vessels moving through body of water, are functions of the ships speeds through the water. For this analysis, it will be assumed that the propulsion from the SLICE adjusts in order to maintain a constant speed for U. Therefore, the surge equation for the SLICE will be ignored and u_1 can be taken as a constant.

The following equations are formed from transformations between coordinate systems and provide the necessary relationships in order to solve the total systems of equations.

$$\dot{X}_1 = u_1 \cos\psi_1 - v_1 \sin\psi_1 \tag{31a}$$

$$\dot{Y}_1 = u_1 \sin\psi_1 + v_1 \cos\psi_1 \tag{31b}$$

$$\dot{X}_2 = u_2 \cos\psi_2 - v_2 \sin\psi_2 \tag{32a}$$

$$\dot{Y}_2 = u_2 \sin\psi_2 + v_2 \cos\psi_2 \tag{32b}$$

also

$$\dot{\psi}_1 = r_1 \tag{33a}$$

$$\dot{\psi}_2 = r_2 \tag{33b}$$

C. SIMULINK TOWING MODEL

The towing model is built using the Matlab Simulink toolbox. The dynamic responses will also be analyzed using Simulink. Simulink allows for continous time modeling of both linear and nonlinear models. Each of the EOMs developed above are modeled in Simulink as superblocks. Each of these equations will be coupled together by the expressions that were built for the tension in the towing connector. One additional transformation needs to be developed since we are interesting in analyzing the maneuvering of the vessels due to towing. The equations of motions are developed for the x and y values being at the center of gravity (assumed midships). The equations below are developed in order to reference ship motions to the point of tow connection rather than center of gravity.

$$x_{c,1} = X_1 - \frac{l_s}{2}\cos\psi_1 \tag{34a}$$

$$y_{c,1} = Y_1 - \frac{l_s}{2}\sin\psi_1 \tag{34b}$$

$$x_{c,2} = X_2 + \frac{l_k}{2}\cos\psi_2 \tag{34c}$$

$$y_{c,2} = Y_2 + \frac{l_k}{2}\sin\psi_2 \tag{34d}$$

The subscript c is used for the tow connection position. Both the tension expression and above expressions for tow connector positions are also modeled with superblocks.

The Simulink towing model is shown in Figure 6. The diagram shows how the Slice sway and yaw EOMs are coupled together by the state variables v_1 and r_1. The Kaimalino surge, sway and yaw EOMs are coupled by the state variables u_2, v_2, and r_2. Each EOM gives an output state that feeds into coordinate transformation equation and results in values of X and Y. The linear towing model couples the motions of the Slice with that of the Kaimalino. Simulink integrator blocks are used to get the state of certain variables. Internal initial conditions are used for the integrator blocks that allow for setting starting values such as position and orientation.

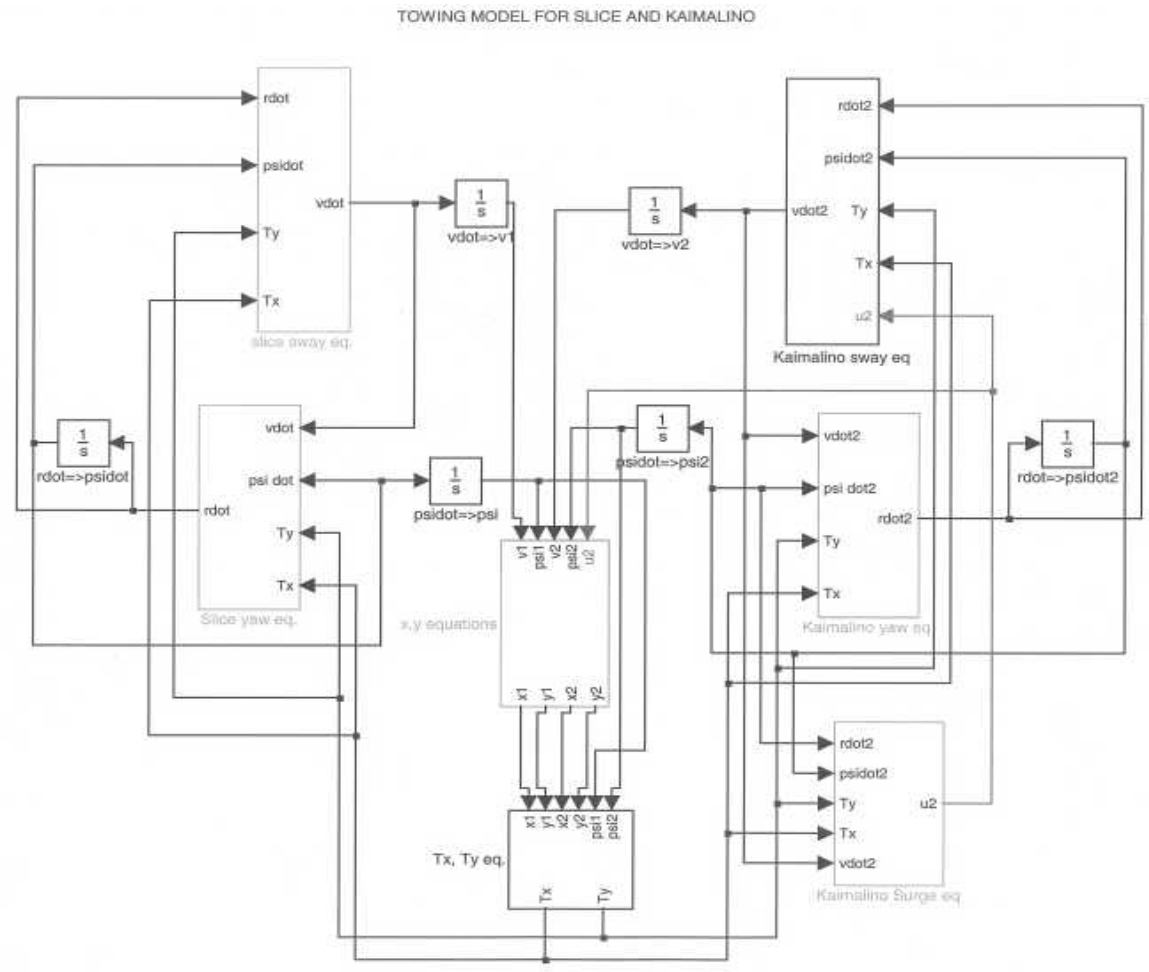

Figure 6. Diagram of Simulink Towing Model for Slice and Kaimalino.

The sway equation of motion for the Slice and Kaimalino is shown in Figures 7 and 8. The diagrams are similar with the exception of rudder force term that is only in the Slice diagram. The longitudinal velocity (u), yaw velocity (r), and yaw acceleration ($\dot{r}$) are input state variables. The lateral velocity is an output state variable and is fed back into the equation using an internal loop. Each one of the state variables is multiplied by respective force or hydrodynamic derivative using gain blocks. The gain blocks also include the dividing through of $m - Y_{\dot{v}}$ term. The variable used for gain blocks are defined in an m-file that initializes the Simulink model. The tension terms are like forcing functions and are added to the system. Each one of the tension terms is multiplied by the gain $m - Y_{\dot{v}}$. The yaw angle (ψ), tension (T_y, T_x), u and r are provided as inputs from other superblocks. The Slice uses a constant u, whereas the Kaimalino uses the input from the surge equation. The equation and diagram are designed to produce the single output of the lateral acceleration $\dot{v}$.

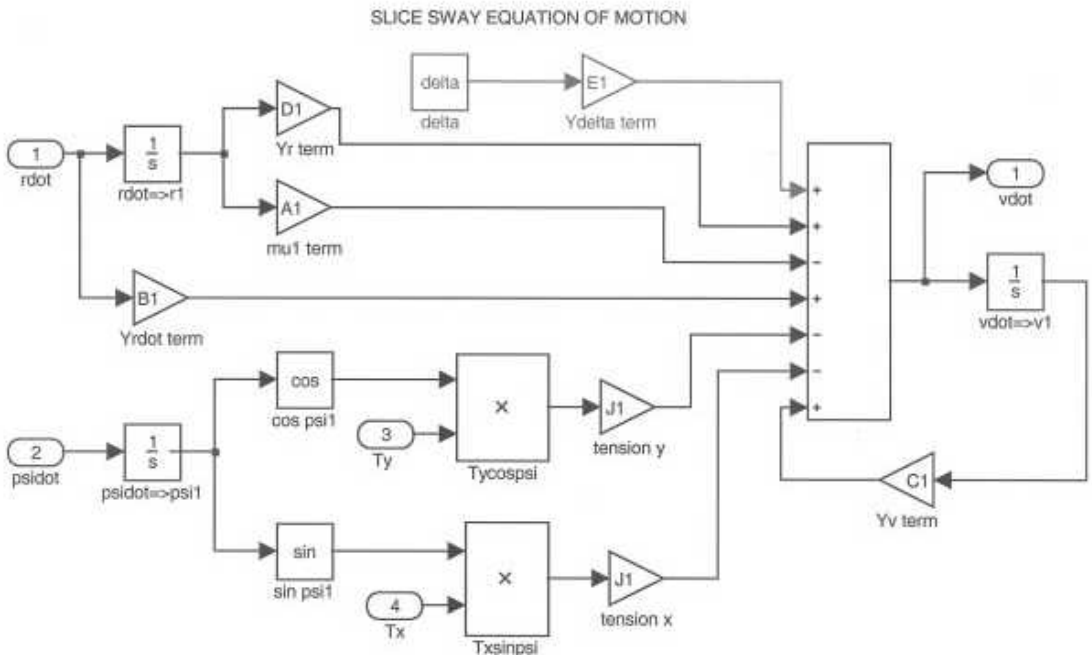

Figure 7. Diagram of Superblock for Slice Sway EOM.

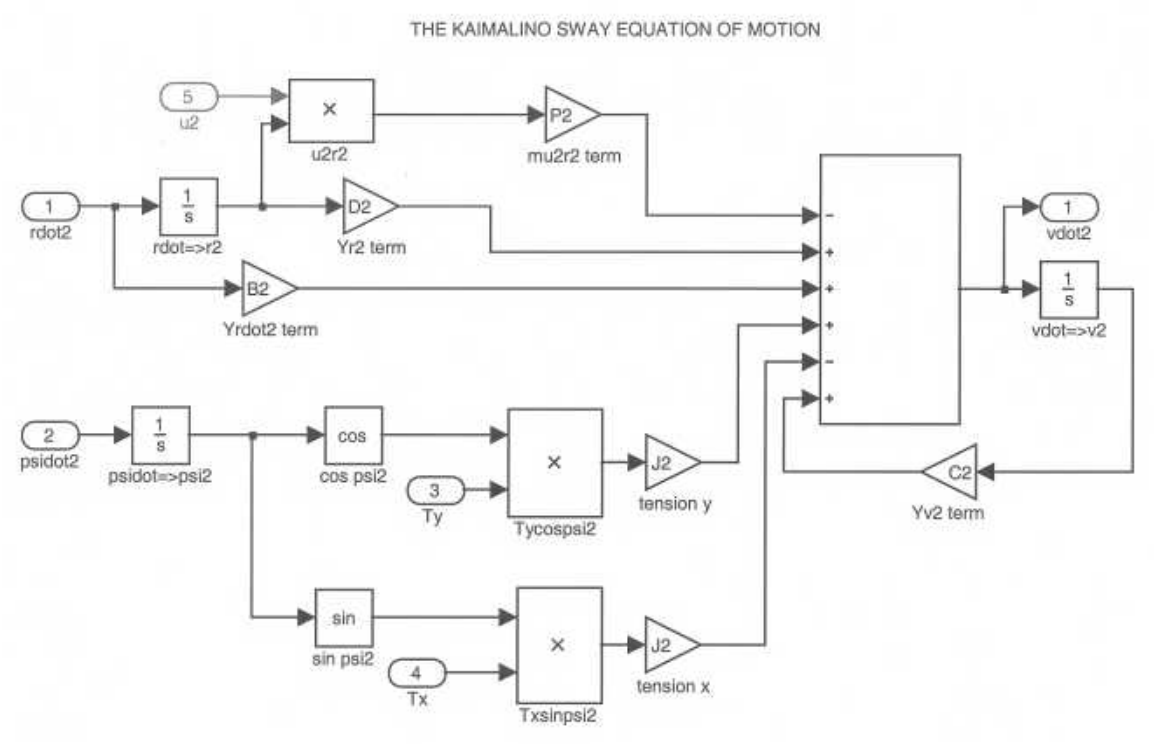

Figure 8. Diagram of Superblock for Kaimalino Sway EOM.

The yaw equations of motion for the Slice and Kaimalino are shown in Figures 9 and 10. The process for building the superblock is similar to that used for the sway equation of motion. The use of gain blocks are used again here to represent the hydrodynamic coefficients divided through by $I_Z - N_{\dot{r}}$ term. The single output for the yaw superblocks is yaw acceleration $\dot{r}$ and the yaw velocity r is fed back into the subsystem using an internal loop.

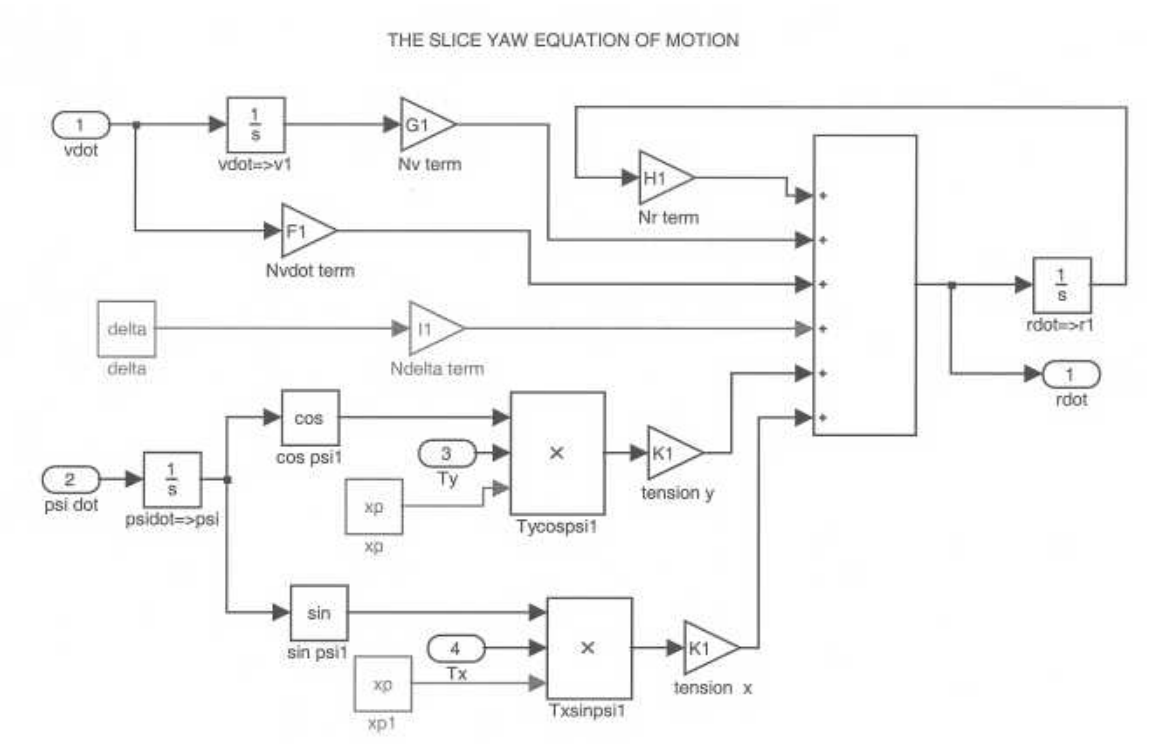

Figure 9. Diagram of Superblock for Slice Yaw EOM.

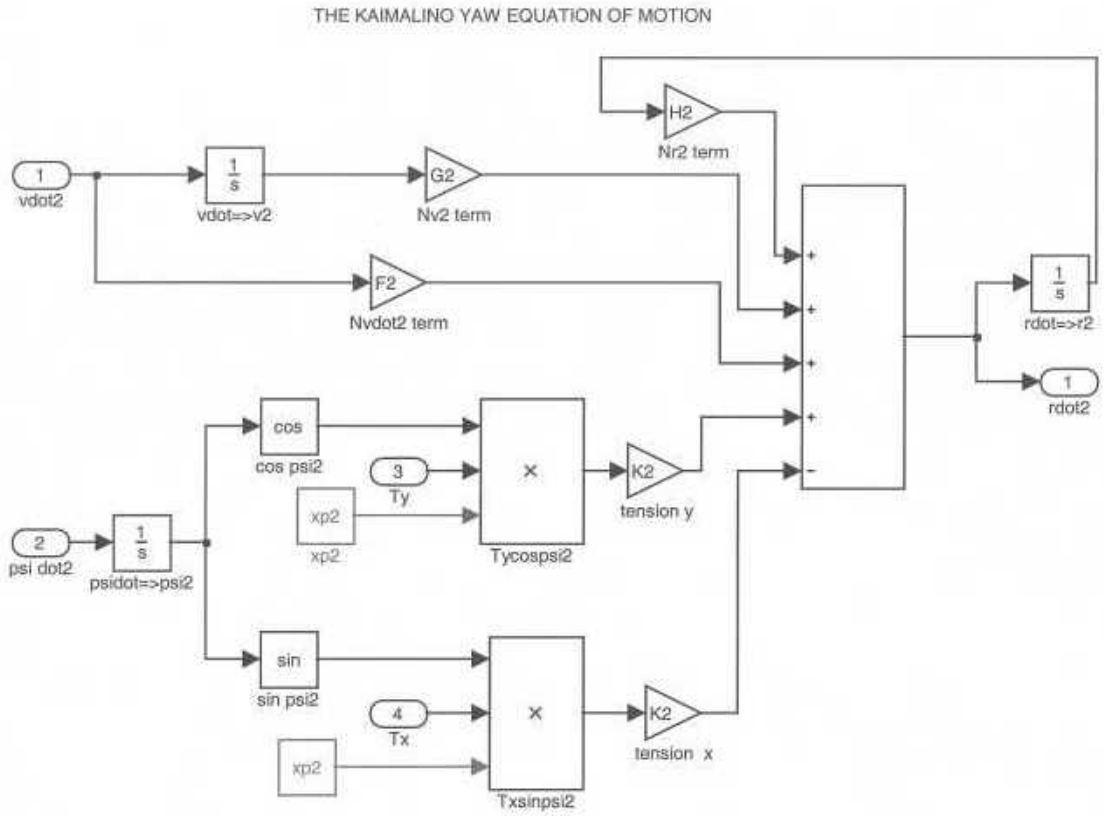

Figure 10. Diagram of Superblock for Kaimalino Yaw EOM.

Figure 11 shows the superblock that represents the Kaimalino surge equation of motion. For this superblock a look-up table was used to model the resistance term in the surge equation. The lookup table matches an input to an output using linear interpolation built into the code. The input for this resistance is the longitudinal speed of the Kaimalino. A graph representing the input and output data is plotted on the lookup table icon. Simulink lookup table can be used for n-dimensions, therefore other resistance forces can be modeled such as wind and current. The other terms and the surge equation are modeled similar to the gain blocks used in the sway and yaw equations of motion. The single output for this superblock is the Kaimalino's longitudinal velocity u.

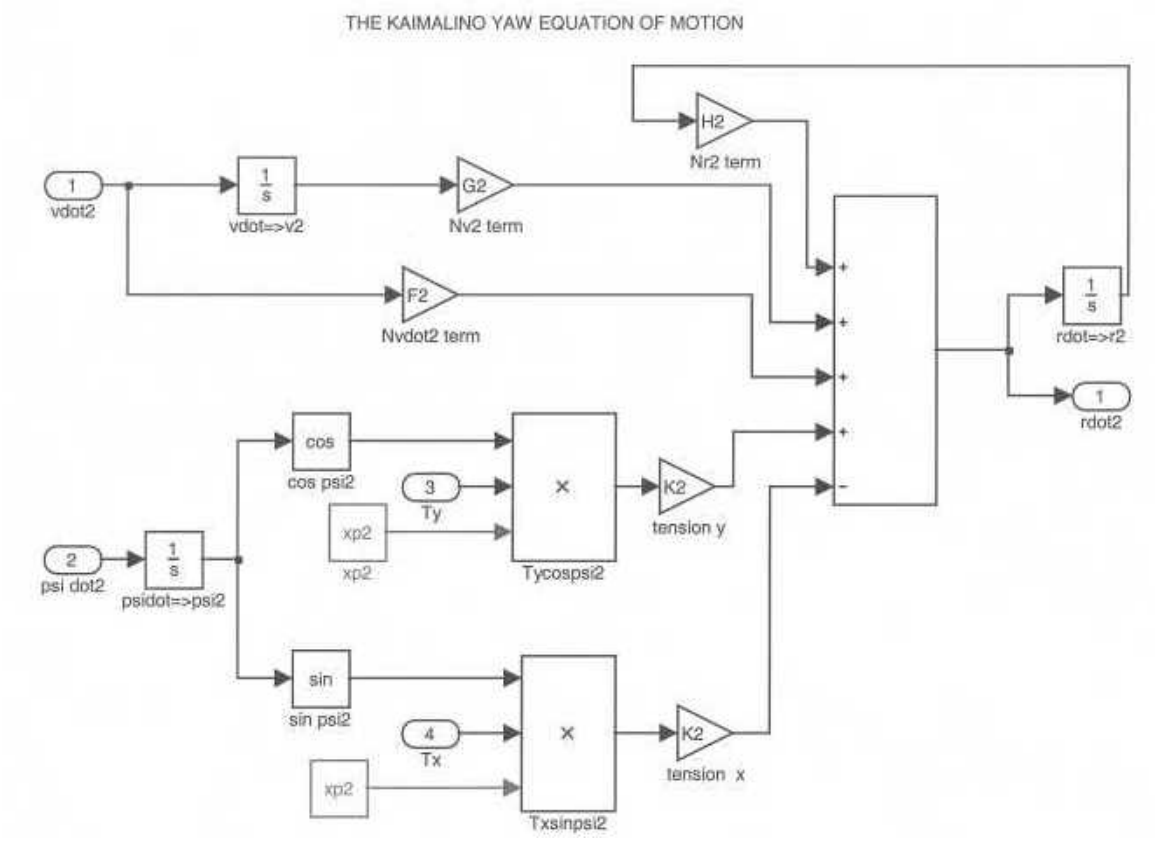

Figure 11. Diagram of Superblock for Kaimalino Surge EOM.

All the variable inputs from the equations of motions for the Slice and Kaimalino are used in the calculation of X and Y. Figure 12 shows this superblock. The

transformation Equations (31a) through (31b) are modeled here. The initial conditions to set up the vessel spacing and length of tow are entered using the integrator blocks for the X and Y states. The values are in terms of ship lengths since all equations of motions were non-dimensionalized.

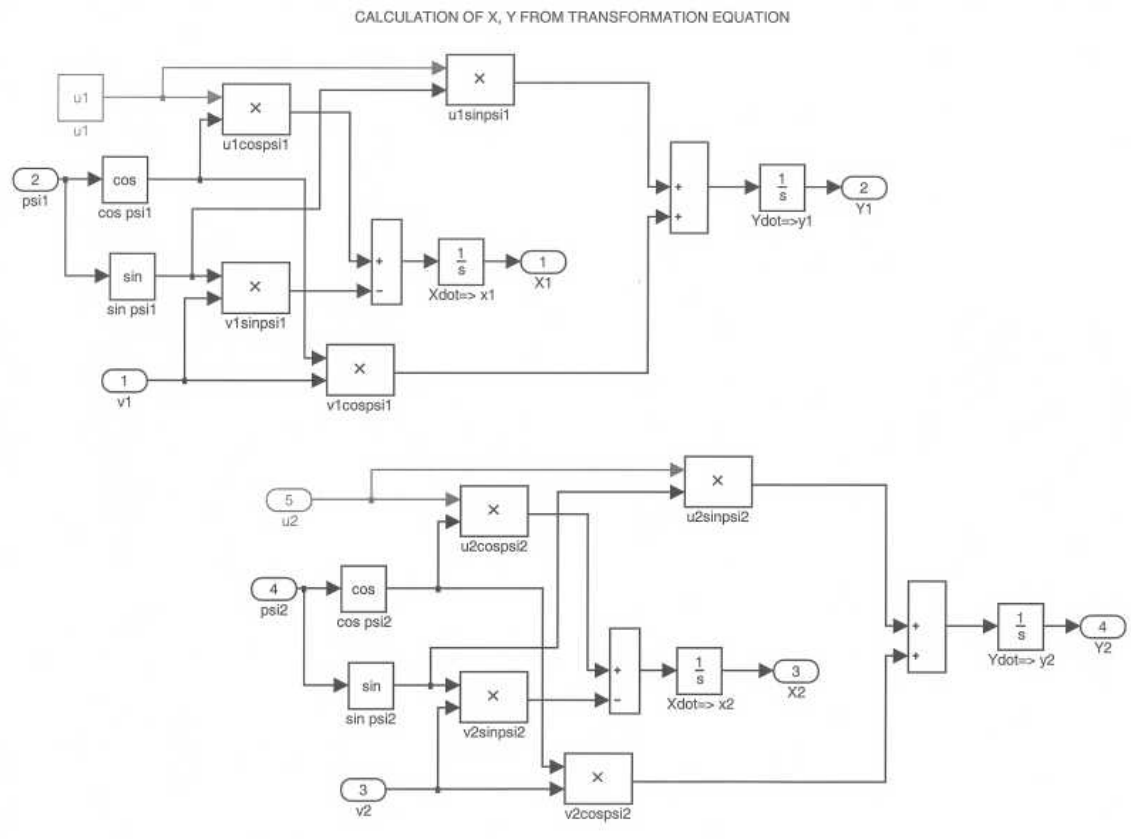

Figure 12. Diagram of Superblock for calculating X and Y for vessels.

The tow-connection is modeled as a linear spring and is represented by the final superblock. The Kaimalino and Slice position variables are used as inputs. Since the EOMs were derived based on x_G and y_G, the position variables need to be referenced to the towing point connection. Equations (34a) through (34d) are modeled here using nondimensional length as the gains. The spring constants K_x and K_y are controllable variables that are initialized in the Matlab m-file. These constants are shown in Figure 13 as gains to the difference in Slice / Kaimalino positions.

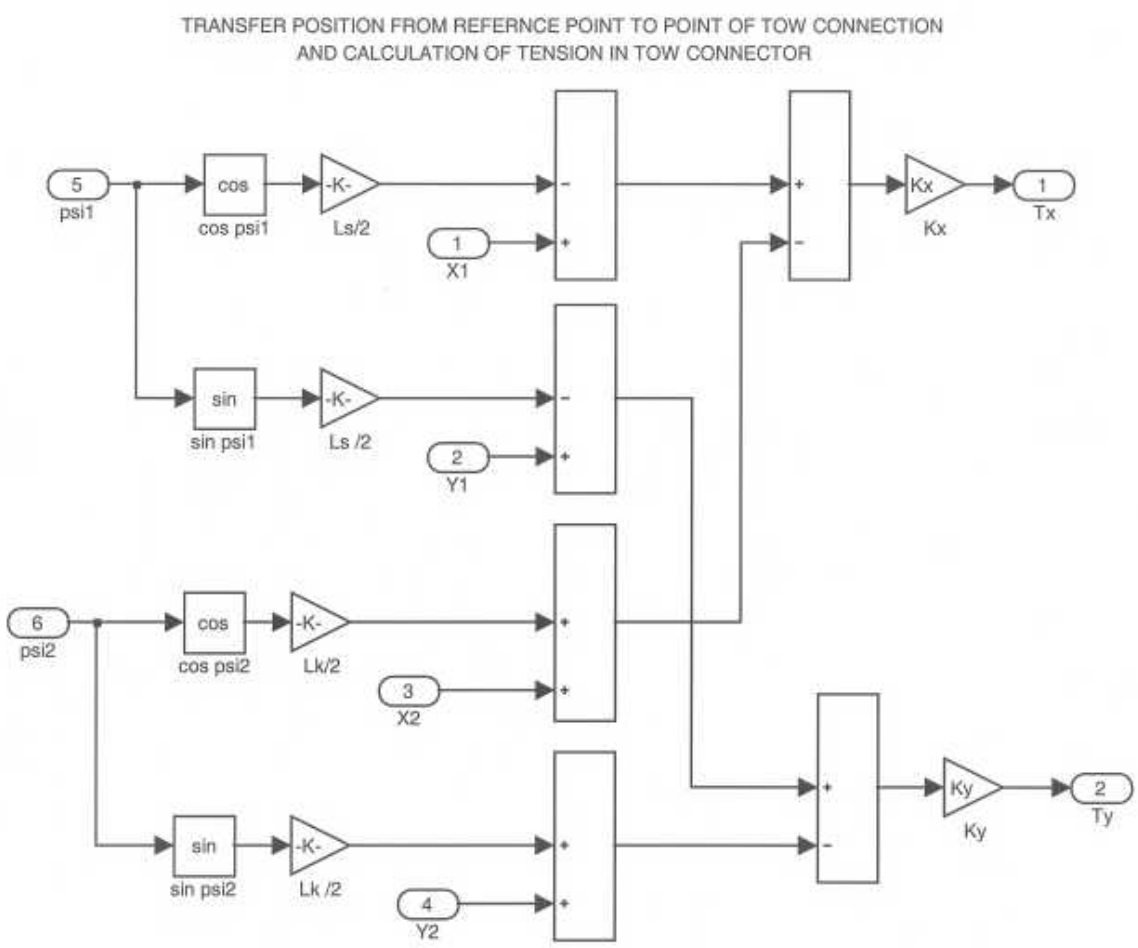

Figure 13. Diagram of Superblock that reference X and Y to the tow connection point and calculates tension.

III. DETERMINATION OF HYDRODYNCAMIC COEFFICIENTS

A. METHODS FOR DETERMINING HYDRODYNAMIC COEFFICIENTS

Theoretical predictions of hydrodynamic coefficients are not exact and still include many assumptions. This is due heavily to the inability of theoretical methods to handle viscous flow situations that occur in the nonlinear range. However correlation with more exact experimental methods has been achieved in the linear prediction range. Because of this problem, tests have been done in order to provide a systematic data base for predicting hydrodynamic coefficients. In Reference [7], the data obtained during tests was coupled with theoretical methods in order to guide semi-empirical methods for calculating hydrodynamic coefficients. These tests were done on certain geometrical shapes, including cylindrical bodies with hemispherical noses and cone shaped tails. This paper uses the semi-empirical methods derived in References [6] and [7].

B. MODEL FOR KAIMALINO PODS AND STRUTS

The Kaimalino pods are modeled as a 78 ft long body of revolution with a 7.4 ft diameter. The nose of the pod is elliptic with a nose length (Ln) of 4.2 ft. The conical tail of the pod is approximately 16 ft. Attached to the pod are the struts that are modeled as 24 x 5.5 ft flat plates. These struts connect the pods to the body of the Kaimalino. The profile is shown below in Figure 14.

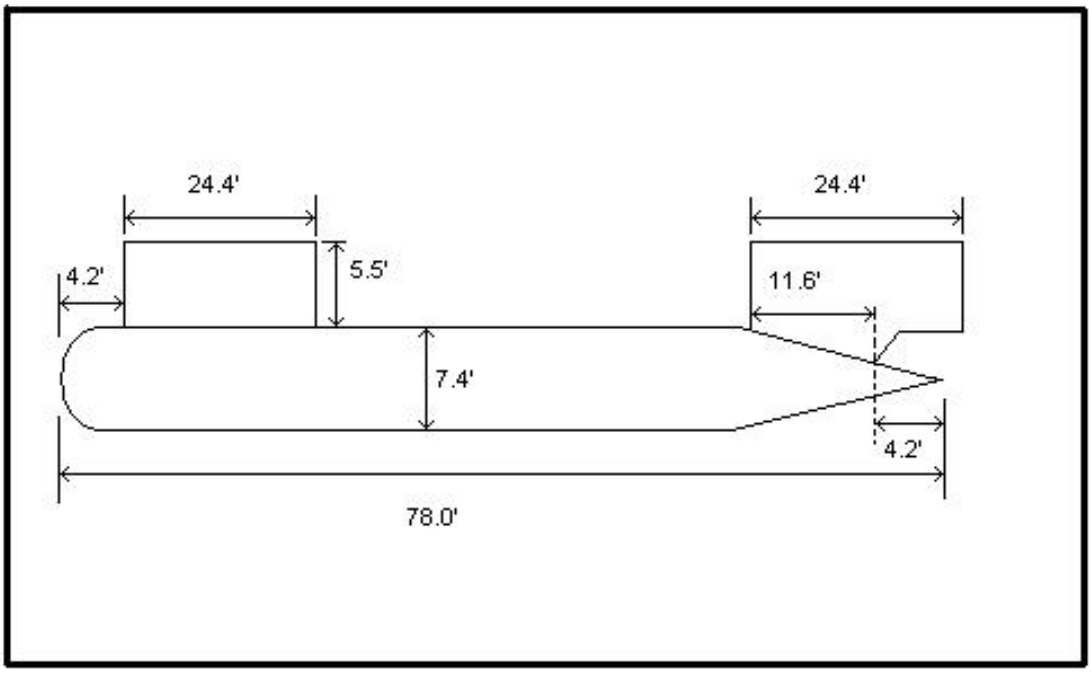

Figure 14. Configuration of one pod with attached struts.

The hydrodynamic coefficients of the Kaimalino pods are calculated using the DATCOM method for each pod without the fins. The midlength of the pod is used as a reference point (x_m). For this model, the reference point is thirty-nine feet (Lb/2). The coefficients will be non-dimensionalized with respect to the pod length (Lb). When summarized later on, the coefficients will be re non-dimensionalized with respect to the length of the Slice model for consistency in the towing simulation.

The struts are modeled as flat plates fixed fins. The struts are referenced to the center of the pod by a distance x_f that is the distance from the quarter chord point of the fin to the center of the pod. After the individual hydrodynamic coefficients for the struts have been obtained, they will be translated and non-dimensionalized with respect to the length of the pod and later re non-dimensionalized with respect to the SLICE length.

C. HYDRODYNAMIC COEFFICIENTS OF KAIMALINO PODS

In order to maintain consistency, the same method that was used for calculating the SLICE model hydrodynamic coefficients is used here in the calculations for the Kaimalino model hydrodynamic coefficients. The models have similar geometry. The

DATCOM method, which is a semi-emperical method was used in the calculation of all the coefficients except for the acceleration hydrodynamic coefficients $Y'\dot{v}$ and $N'\dot{r}$. For these two, the works of Humphrey and Watkinsn [6] was used. The coefficients were calculated from the following equations using DATCOM method

$$(Y'v)_{pod} = \frac{-S_b}{l^2}[C_{L\alpha} + C_{Do}] \tag{35}$$

$$(N'v)_{pod} = \frac{S_b C_{m\alpha}}{l^2} \tag{36}$$

$$(Y'r)_{pod} = \frac{S_b}{l^2} C_{L\alpha}\left(1 - \frac{x_m}{l}\right) \tag{37}$$

$$(N'r)_{pod} = \frac{S_b}{l^2} C_{mq} \tag{38}$$

where S_b is the maximum cross-sectional area of the pod and l is the total length of the pod. $C_{L\alpha}$ is the slope of the lift curve. C_{Do} is the drag coefficient of an elliptical form at a zero angle of attack. $C_{m\alpha}$ is the slope of the yawing moment curve. C_{mq} is the slope of the yawing moment curve for the plansform based on effective area. The slopes and values where calculated with the following equations

$$C_{L\alpha} = 2(k_2 - k_1)\frac{S_v}{S_b} \tag{39}$$

where k_2 and k_1 are the Lamb's coefficients of inertia for a prolate ellipsoid in axial and cross sectional flow respectively. S_v is the cross sectional area at a point l_v. L_v is the point on the pod where flow becomes viscous. The empirical relation for calculating l_v is

$$l_v = 0.378 l_B + 0.527 l_{ms} \tag{40}$$

L_{ms} is the distance from the nose of the pod to the point of maximum slope. For this model, L_{ms} is equal to L_B, the total length of the pod.

$$C_{M\alpha} = 2\left(\frac{k_2 - k_1}{S_b l}\right)\int_0^{l_v} \frac{dS}{dx}(x_m - x)dx \tag{41}$$

$$C_{mq} = C_{m\alpha}\left[\frac{\left(1-\frac{x_m}{l}\right)^2 - \left(\frac{V}{S_{tb*}l}\right)\left(\frac{l_c}{l} - \frac{x_m}{l}\right)}{\left(1-\frac{x_m}{l}\right) - \left(\frac{V}{S_{tb*}l}\right)}\right] \tag{42}$$

Here V is the volume of the submerged body, l_c is the distance from the nose to the center of buoyancy, and S_{tb} is the area of the truncated base at l_v.

The acceleration hydrodynamic coefficients are calculated as follows using the works of Humphrey and Watkinson [6].

$$(Y'\dot{v})_{pod} = \frac{k_2 V}{0.5 l^3} \tag{43}$$

$$(N'\dot{r})_{pod} = -k_b I'_{zdf} + Y'\dot{v}\left(\frac{l_{cb} - l_{cg}}{l^2}\right) \tag{44}$$

where k_b is Lamb's coefficient of added moment of inertia for a prolate ellipsoid body. I'_{zdf} is the mass moment of inertia of the displaced fluid about the z-axis. Table 3 shows the coefficients for single pods for the Kaimalino and the results obtained by William Wolkerstorfer for a SLICE single pod.

Coefficients	SLICE POD	KAIMALINO POD
Y'_v	-0.016244	-0.0592
Y'_r	-0.002498	-0.0014
N'_v	-0.038754	-0.0086

N'_r	-0.006396	-0.0087
$Y'_{\dot{v}}$	-0.044189	-0.0407
$Y'_{\dot{r}}$	0.0	-0.0001
$N'_{\dot{v}}$	0.0	0.0001
$N'_{\dot{r}}$	-0.001799	-0.0045

Table 3. Hydrodynamic coefficients for SLICE and Kaimalino pods.

D. HYDRODYNAMIC COEFFICIENTS OF KAIMALINO STRUTS

Theoretical predictions for hydrodynamic coefficients for fixed fins in the linear range are presented in [3]. The process for theoretical prediction of forces and moments in the nonlinear range is still an area under development. One of the assumptions that is made in linear theory is that the effects of the ship's hull on its fixed fins is negligible. For traditional hulls, that assumption is not really justified especially in situations of tight maneuvers. For the Kaimalino hull, the assumption is more justified because of the swath hull design. The hydrodynamic coefficients for the fixed fin are as follows.

$$(Y_v)_{fin} = -A\left(\frac{\partial C_L}{\partial \beta} + C_D\right) \tag{45}$$

$$(N'_v)_{fin} = Y'_{v*} x'_f \tag{46}$$

$$(Y'_r)_{fin} = x'_{f*} Y'_v \tag{47}$$

$$(N'_r)_{fin} = Y'_{V*} x'^2_f \tag{48}$$

where A' is the fin area that is non-dimensionalized by the length times the draft. $\partial C_L/\partial\beta$ is the slope of the lift-curve where β is the angle of attack at the fin. C_D is the drag coefficient at zero angle of attack. C_D is small compared to the lift-curve slope for fixed fins therefore it is ignored. Equations (45) through (52) are derived from

summation of forces and moments about point x_m with x_f taken as the distance from the quarter chord point to x_m.

$$(Y'_{\dot{v}})_{fin} = \frac{-4\pi b' A'_f}{\sqrt{a^2{}_G + 1}} \tag{49}$$

$$(N'_{\dot{v}})_{fin} = Y'_{\dot{v}} * x'_f \tag{50}$$

$$(Y'_{\dot{r}})_{fin} = Y'_{\dot{v}} * x'_f \tag{51}$$

$$(N'_{\dot{r}})_{fin} = Y'_{\dot{v}} * x'^2{}_f \tag{52}$$

where b is the geometric span and a_G is the geometric aspect ratio b^2/A_f. The effective aspect ratio of a fin attached to ship's hull becomes $2a_G$.

The total contribution for one pod/fins configuration is now calculated by simply adding the contributions from both forward and aft fins to the pod.

$$(Y'_V) = (Y'_V)_{pod} + (Y'_V)_{fin,\,aft} + (Y'_V)_{fin,\,fwd} \tag{53a}$$

$$(Y'_r) = (Y'_r)_{pod} + (Y'_r)_{fin,\,aft} + (Y'_r)_{fin,\,fwd} \tag{53b}$$

$$(N'_v) = (N'_v)_{pod} + (N'_v)_{fin,\,aft} + (N'_v)_{fin,\,fwd} \tag{53c}$$

$$(N'_r) = (N'_r)_{pod} + (N'_r)_{fin,\,aft} + (N'_r)_{fin,\,fwd} \tag{53d}$$

$$(Y'_{\dot{V}}) = (Y'_{\dot{V}})_{pod} + (Y'_{\dot{V}})_{fin,\,aft} + (Y'_{\dot{V}})_{fin,\,fwd} \tag{53e}$$

$$(Y'_{\dot{r}}) = (Y'_{\dot{r}})_{pod} + (Y'_{\dot{r}})_{fin,\,aft} + (Y'_{\dot{r}})_{fin,\,fwd} \tag{53f}$$

$$(N'_{\dot{v}}) = (N'_{\dot{v}})_{pod} + (N'_{\dot{v}})_{fin,\,aft} + (N'_{\dot{v}})_{fin,\,fwd} \tag{53g}$$

$$(N'_{\dot{r}}) = (N'_{\dot{r}})_{pod} + (N'_{\dot{r}})_{fin,\,aft} + (N'_{\dot{r}})_{fin,\,fwd} \tag{53h}$$

E. COMPLETE HYDRODYNAMIC DERIVATIVES FOR THE SLICE AND KAIMALINO CONFIGURATIONS

The final step in calculating the hydrodynamic coefficients is to translate the contributions for each pod/strut configuration. This is achieved by summing forces and moments about a common reference point on the vessel. Adapting the equations derived in Principles of Naval Architecture [3] results in the following equations.

$$(Y'_v) = (Y'_v) \tag{54}$$

$$(Y'_r) = (Y'_v)x'_f + (Y'_r) \tag{55}$$

$$(N'_v) = (Y'_v)x'_f + (N'_v) \tag{56}$$

$$(N'_r) = (Y'_r)x'_f + (Y'_v)x'^2_f + (N'_v)x'_f + (N'_r) \tag{57}$$

where x'_f is taken as the distance from amidship the vessel to the center point of the pods.

Similar logic is repeated for the acceleration hydrodynamic derivatives.

$$(Y'_{\dot{v}}) = (Y'_{\dot{v}}) \tag{58}$$

$$(Y'_{\dot{r}}) = (Y'_{\dot{v}})x'_f + (Y'_{\dot{r}}) \tag{59}$$

$$(N'_{\dot{v}}) = (Y'_{\dot{v}})x'_f + (N'_{\dot{v}}) \tag{60}$$

$$(N'_{\dot{r}}) = (Y'_{\dot{r}})x'_f + (Y'_{\dot{v}})x'^2_f + (N'_{\dot{v}})x'_f + (N'_{\dot{r}}) \tag{61}$$

The hydrodynamic coefficients were then non-dimensionalized with respect to the characteristic length of the SLICE vessel in order to maintain continuity for the towing simulation. Assuming similarity for port and starboard pod/strut configuration, the coefficients were then multiplied by two. A summary of both Kaimalino hydrodynamic coefficients and SLICE coefficients that were calculated in previous thesis work are provided in the table below.

Hydrodynamic Coefficients	Kaimalino (w/o rudders)	SLICE (w/o rudders)
Y'_v	-0.1183	-0.078930
Y'_r	-0.0042	-0.004044
N'_v	-0.0187	-0.016428
N'_r	-0.0176	-0.010332
$Y'_{\dot{v}}$	-0.0184	-0.051328
$Y'_{\dot{r}}$	-0.0011	0.005617
$N'_{\dot{v}}$	-0.0008489	-0.001945
$N'_{\dot{r}}$	-0.0090	-0.00564

Table 4. Complete hydrodynamic coefficients for SLICE and Kaimalino vessels.

IV. RESULTS AND DISCUSSION

A. INITIAL MODEL TEST

Initially, we conducted the 1st set of runs in order to validate the simulation model. For this run, the towing vessel was on the same path as the lead vessel. The initial conditions were as follows.

Slice initial speed = 15 knots

Kaimalino initial speed = 13.5 knots

Slice initial yaw angle = 0

Kaimalino initial yaw angle = 0 degrees

Kaimalino offset from path = 0

K_x is varied while K_y is held constant, and the longitudinal offset is observed. Figure 15 shows the results of these simulation runs. The trend shows a decreasing offset for higher values of stiffness in the K_x parameter as expected. The non-dimensional value K_x value of 0.06 corresponds to a near rigid towing connection where there is very little deformation based on the stiffness.

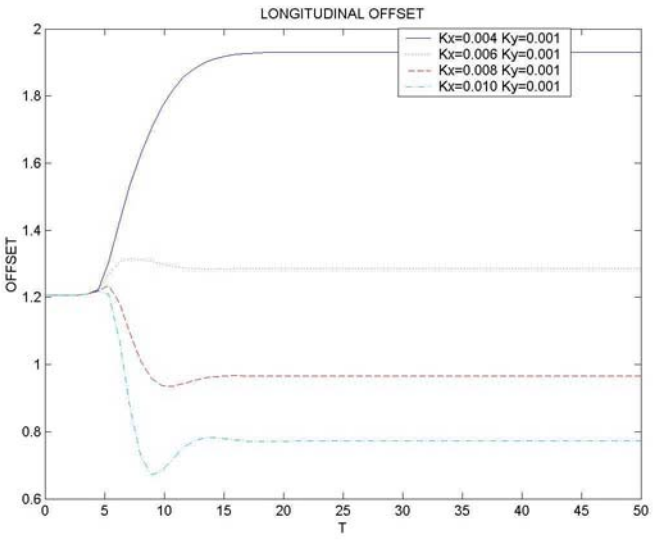

Figure 15. Longitudinal Offset observation while varying K_x for 3rd set of simulation runs initial conditions.

B. DIRECTIONAL STABILITY

Various simulation runs were conducted in order to analyze the directional stability of the towing model. There are different kinds of motion stability when dealing with surface vessels. In general, motion stability is the ability of the vessel to retain as much of the initial state of equilibrium in its final path after some disturbance has occurred. For directional stability, the vessel's final path will retain the straight line motion it initially had as well as its initial direction. A vessel may oscillate after the disturbance or may transition smoothly back to its original state. The latter is obviously preferred since it corresponds to a more stable vessel.

In the simulation runs conducted for this paper, two sets of initial conditions were applied. For these runs, the vessel being towed has experienced a disturbance and is offset from the initial path set by the lead vessel. The lateral offset is observed to study if the vessel is directionally stable or not. For each of these sets, different combinations of stiffness coefficients are applied. For the 1st set of runs, the initial conditions are as follows.

Slice initial speed = 15 knots

Kaimalino initial speed = 13.5 knots

Slice initial yaw angle = 0

Kaimalino initial yaw angle = 0

Kaimalino Offset from path = 0.1 (non-dimensionalized to SLICE length)

Figures 16 and 17 show the results of varying K_y while holding K_x constant.

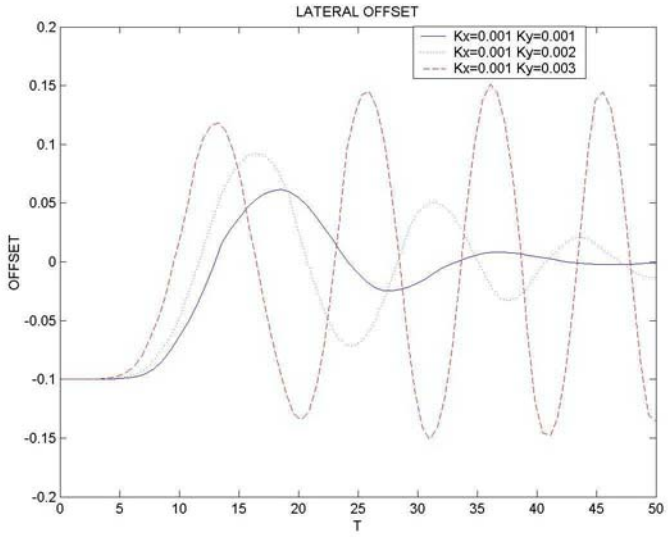

Figure 16. Lateral offset for varying K_y for 1st set initial conditions.

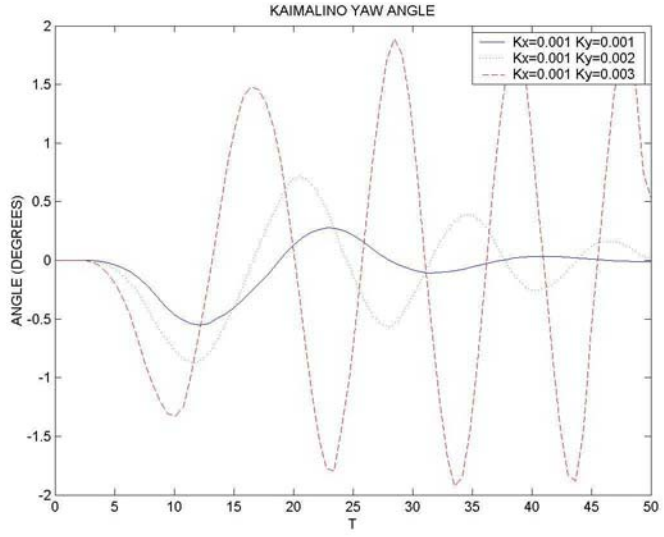

Figure 17. Kaimalino yaw angle for varying K_y for 1st set initial conditions.

From the figures it is evident that as K_y increases, the lateral offset and the yaw angle oscillate more. This indicates that the system will eventually go unstable if K_y is increased too much while holding K_x constant. The oscillation is around the zero offset which is the critical point to be used in an eigenvalue analysis.

The next two figures show the results of varying K_x while holding K_y constant.

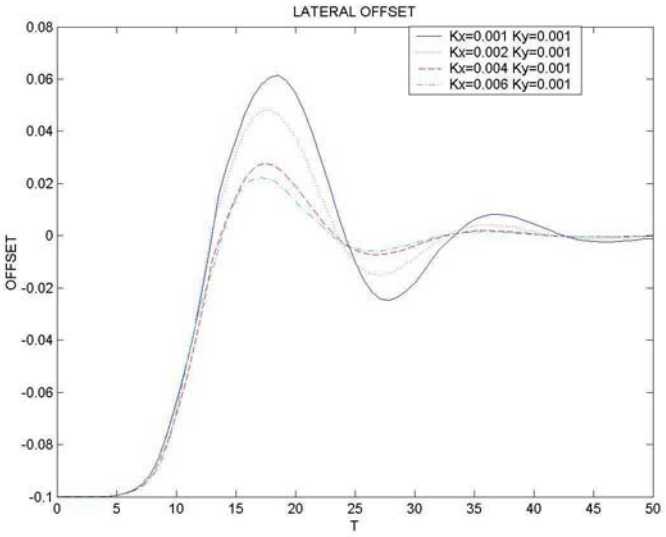

Figure 18. Lateral offset for varying K_x for 1st set initial conditions.

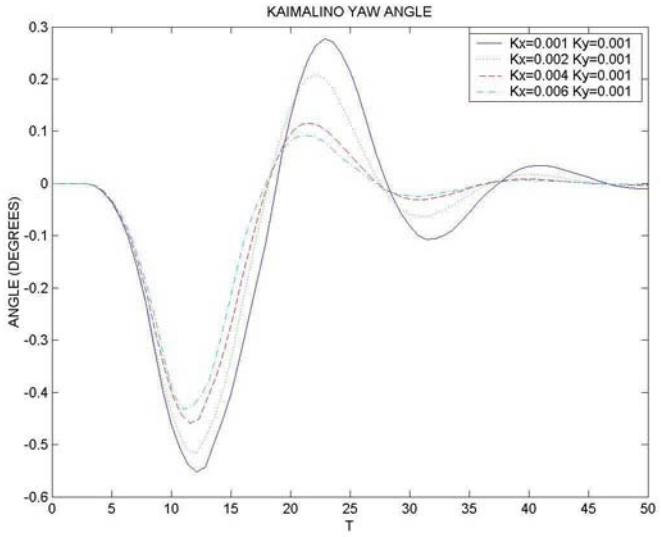

Figure 19. Kaimalino yaw angle for varying K_x for 1st set initial conditions.

Now for an increasing K_x value, there is significantly less oscillation and the systems is more stable at the higher values.

The last results for the set of initial conditions are for varying K_x and K_y at the same time.

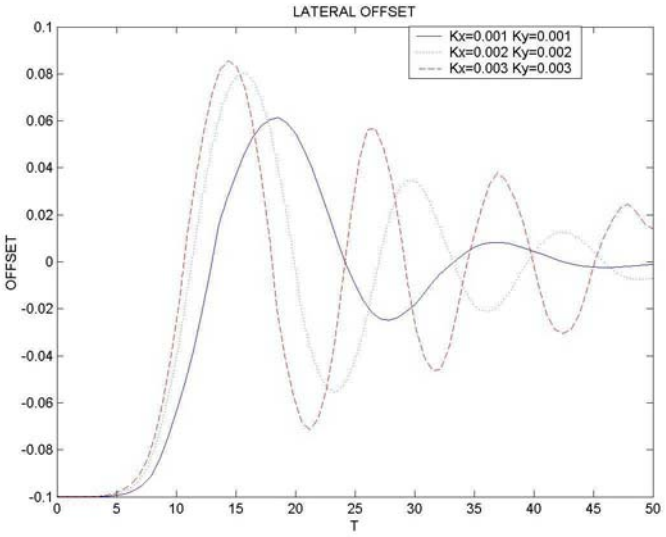

Figure 20. Lateral offset for varying K_x and K_y for 1st set initial conditions.

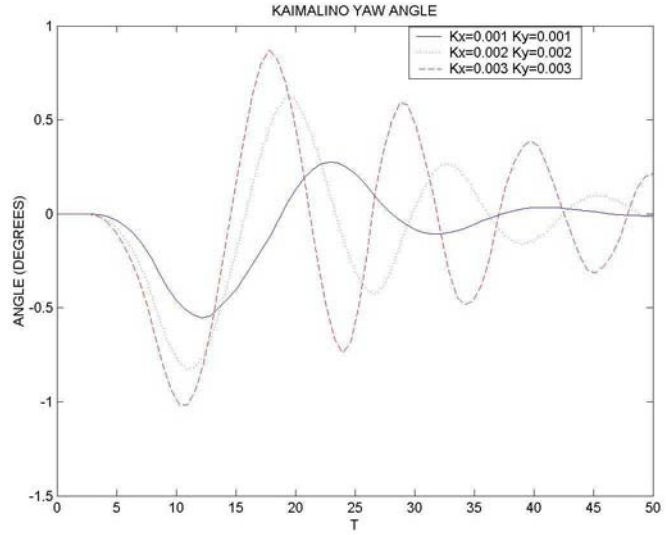

Figure 21. Kaimalino yaw angle for varying K_x and K_y for 1st set initial conditions.

The figures show that when increasing both K_x and K_y, the directional stability decreases. However, increasing K_x, slows down the oscillations that were occurring in the case of increasing K_y only.

For the 2nd set of runs, the initial conditions are as follows.

Slice initial speed = 15 knots

Kaimalino initial speed = 13.5 knots

Slice initial yaw angle = 0

Kaimalino initial yaw angle = 10 degrees

Kaimalino Offset from path = 0

Figures 22 through 27 show the results of different combinations of stiffness coefficients for the 2nd set of initial conditions. The trend for the results is similar to what was observed in the 1st set of simulation runs. For the Kaimalino yaw angles, the results show that the angles return to the critical point (0 offset) either smoothly or with oscillation. Either case the system has some measure of stability for the different stiffness coefficients.

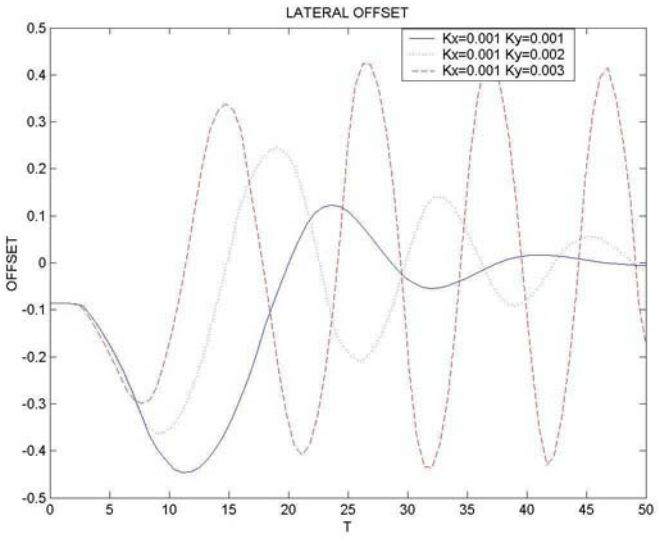

Figure 22. Lateral offset for varying K_y for 2nd set initial conditions.

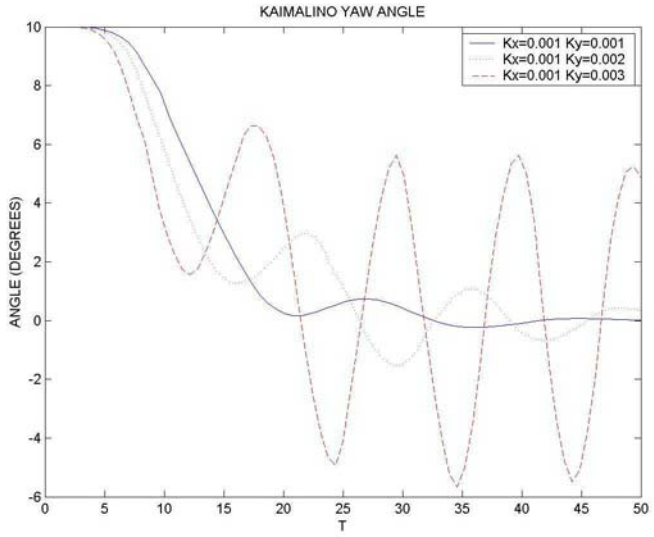

Figure 23. Kaimalino yaw angle for varying K_y for 2nd set initial conditions.

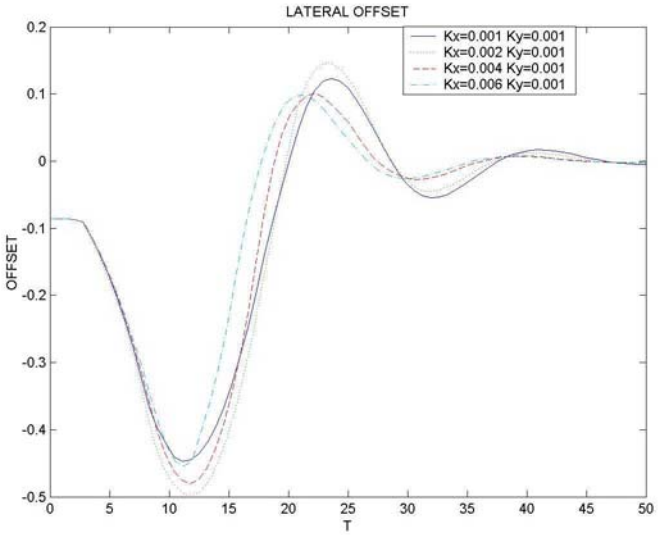

Figure 24. Lateral offset for varying K_x for 2nd set initial conditions.

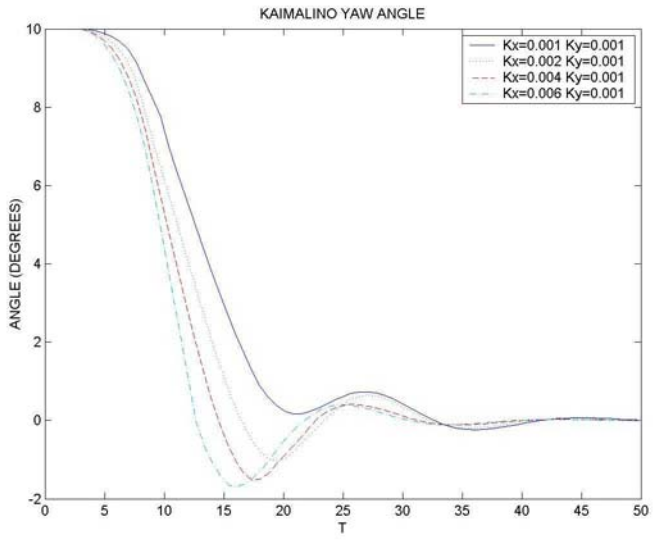

Figure 25. Kaimalino yaw angle for varying K_x for 2nd set initial conditions.

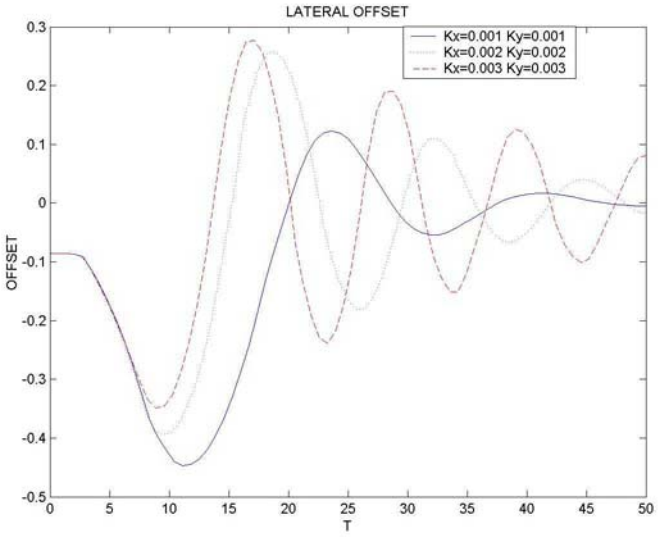

Figure 26. Lateral offset for varying K_x and K_y for 2nd set initial conditions.

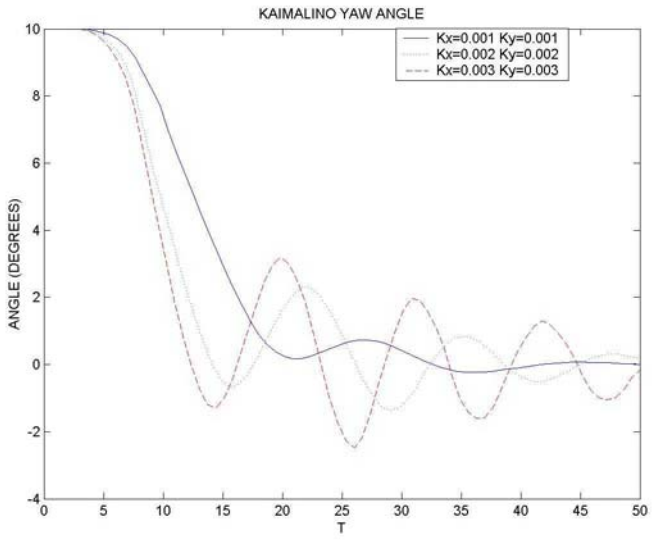

Figure 27. Kaimalino yaw angle for varying K_x and K_y for 2nd set initial conditions.

THIS PAGE INTENTIONALLY LEFT BLANK

V. CONCLUSIONS

A simulation model has been developed that represents the coupled dynamics of two vessels in a towing operation. This nonlinear time-dependent simulation model is useful for course stability analysis of more sophisticated towing systems. The model takes into account the effects of towline dynamics through a set of generalized stiffness coefficients. Based on the results obtained from the simulations runs presented in this paper, it is feasible to have a near rigid towing connection for the Slice towing the Kaimalino in close proximity. However, the results seem to indicate that the need for some flexibility in the longitudinal direction for the stiffness or even a controlled attachment point which would allow for longitudinal motion of the towing connector.

As a recommendation for further research, a study of the eigenvalues using a perturbation analysis near the critical points should be conducted in order to find the range of K_x and K_y values that make the system stable or unstable

THIS PAGE INTENTIONALLY LEFT BLANK

APPENDIX A. MATLAB PROGRAM FOR CALCULATION OF HYDRODYNAMIC COEFFICIENTS FOR SINGLE POD/STRUT CONFIGURATION AND COMPLETE HYDRODYNAMIC COEFFICIENTS.

```
%LT Garrett Jones
%Thesis Work
%Kaimalino Hydrodynamic Coefficients
%Following programs are developed to calculation Hydrodynamic Coefficients (HCs)
%for Kaimalino using the DATCOM method and works of Humphrey and Watkinson.
%This method was used by William Wolkerstorger in calculating HCs for the SLICE

%Single Pod calculations

%Initial Values
gamma=62.4; %lbf/ft^3
g=32.2; %ft/sec^2
rho =gamma/g;
r=4; % radius of pod
lb=78; % base length
lms=78; % length to point of maximum slope
ln=4; % nose length
lf=62; % length of forebody
lc=lb-lf; % length of conical tail
lpmb=lf-ln; % length of parallel midbody
xm=39; % reference point for calculations
d=7.4;

% Calculations of sectional areas, curve slopes, and coefficients needed
% needed for determining HCs
lv=0.378*lb+0.527*lms; % length where flow becomes viscous
Sv=pi*(r*(lb-lv)/lc)^2;
```

```
Sb=pi*r^2;
k2=.963269;
k1=.019066;
kb =0.892252;
Cla=2*(k2-k1)*(Sv/Sb);
Cd=0.29;
INT1=(-0.5*pi*d^2/ln^2)*((1/3)*ln^3-(1/2)*ln^3+xm*ln^2-(1/2)*xm*ln^2);
INT2=(.5*pi*d^2/lc^2)*[(-.5*lv^2*lc+(1/3)*lv^3-.5*lv^2*lf+xm*lc*lv-.5*xm*lv^2+...
    xm*lf*lv)-(-.5*lf^2*lc+(1/3)*lf^3-.5*lf^3+xm*lc*lf-.5*xm*lf^2+xm*lf^2)];
Cma=(2*(k2-k1)/(Sb*lb))*(INT1+INT2);
Stb=(d/lc)*(lc*lb-(1/2)*lb^2+lf*lb-lc*lv+(1/2)*lv^2-lf*lv);
V=(pi*d^2/4)*(ln-ln/3+lpmb+lb^3/(3*lc^2)-lb^2*lf/lc^2-lf^3/(3*lc^2)+...
     lb*lf^2/lc^2);
lcb=[(pi*d^2/4)*((2/3)*ln^2-ln^2/4+0.5*lpmb^2+lb^4/(12*lc^2)-lb^2*...
     lf^2/(2*lc^2)-lf^4/(4*lc^2)+2*lb*lf^3/(3*lc^2))]/V;
lcg =lcb;
Cmq=Cma*[((1-xm/lb)^2-(V/(Stb*lb))*((lcb/lb)-(xm/lb)))/((1-xm/lb)-(V/...
     (Stb*lb)))];
Clq=Cla*(1-xm/lb);
Iydf =(rho*pi*d^2/4)*[(3*ln^3/10)-(5*xm*ln^2/6)+(2*xm^2*ln/3)+xm^2*lpmb-...
     xm*lpmb^2+(lpmb^3/3)+(1/lc^2)*((lb^5/30-xm*lb^4/6+xm^2*lb^3/3)-...
     (lf^5/5-xm*lf^4/2-lb*lf^4/2+xm^2*lf^3/3+lb^2*lf^3/3+4*xm*lb*lf^3/3-...
     xm^2*lb*lf^2-xm*lb^2*lf^2+xm^2*lb^2*lf))];

% Calculations of HCs
Yv=-(Sb/lb^2)*(Cla+Cd);
Yr = -(Sb*Clq)/lb^2;
Nv=(Sb/lb^2)*Cma;
Nr = -(Sb*Cmq)/lb^2;
Yvdot = -(k2*V)/(0.5*lb^3);
Nrdot = (-kb*Iydf/(0.5*rho*lb^5))+Yvdot*((lcb-lcg)/lb);
HCP(1)=Yv;
HCP(2)=Yr;
```

```
HCP(3)=Nv;
HCP(4)=Nr;
HCP(5)=Yvdot;
HCP(6)=0;
HCP(7)=0;
HCP(8)=Nrdot;
```

```
%LT Garrett Jones
%Thesis Work
%Kaimalino Hydrodynamic Coefficients

% Struts Calculations
%--------------------------------------------------------------------------
% Initial Values
LB = 78; %length of pod
Lbp = 81.8; %length between perpendiculars
T=14; % draft
xm=39;
xf=28.8;  %distance from xm to quarter chord fwd fin
xf2=-29.2; %distance from xm to quarter chord aft fin
b=5.5;
c=24;

% Calculation of areas, aspect ratios, and curve slopes needed for determing HCs
A=b*c;
ag=2*(b/c);
a=ag;
Cla=(0.9*pi*2*a)/(sqrt(a^2+4)+1.8);
Cmcl=1/2-((1.11*sqrt(ag^2+4)+2)/(4*ag+2));
Cmc4=(.25-Cmcl)*Cla;
Xf=xf;
Xf2=xf2;

% HCs calculations for single strut
Yv=-abs(A*Cla/(LB*T));
Yr=(Xf/LB)*Yv;
Nv=Yr;
Nr=(Xf/LB)^2*Yv;
Yvdot=-(2*pi*c*b^2)/((LB^2*T)*sqrt(ag^2+1));
```

```
Yrdot=-(Xf/LB)*Yvdot;
Nvdot=(Xf/LB)*Yvdot;
Nrdot=(Xf/LB)^2*Yvdot;

Yv2=-abs(A*Cla/(LB*T));
Yr2=(Xf2/LB)*Yv2;
Nv2=Yr2;
Nr2=(Xf2/LB)^2*Yv2;
Yvdot2=-(2*pi*c*b^2)/((LB^2*T)*sqrt(ag^2+1));
Yrdot2=-(Xf2/LB)*Yvdot2;
Nvdot2=(Xf2/LB)*Yvdot;
Nrdot2=(Xf2/LB)^2*Yvdot2;

HCS(1) = Yv;        HCS2(1) = Yv2;
HCS(2) = Yr;        HCS2(2) = Yr2;
HCS(3) = Nv;        HCS2(3) = Nv2;
HCS(4) = Nr;        HCS2(4) = Nr2;
HCS(5) = Yvdot;     HCS2(5) = Yvdot2;
HCS(6) = Yrdot;     HCS2(6) = Yrdot2;
HCS(7) = Nvdot;     HCS2(7) = Nvdot2;
HCS(8) = Nrdot;     HCS2(8) = Nrdot2;

%----------Non-dimensionalize and combining strut and pod coefficients----------
HC(1)= HCP(1)(LB/Lbp)^2 + 2HCS(1)*(LB*T)/Lbp^2+ 2HCS2(1)(LB*T)/Lbp^2;
HC(2)= HCP(2)(LB/Lbp)^3 + 2HCS(2)(LB^2*T)/Lbp^3+ 2HCS2(2)(LB^2*T)/Lbp^3;
HC(3)= HCP(3)(LB/Lbp)^3 + 2HCS(3)(LB^2*T)/Lbp^3+ 2HCS2(3)(LB^2*T)/Lbp^3;
HC(4)= HCP(4)(LB/Lbp)^4 + 2HCS(4)(LB^3*T)/Lbp^4+ 2HCS2(4)(LB^3*T)/Lbp^4;
HC(5)= HCP(5)(LB/Lbp)^3 + 2HCS(5)(LB^2*T)/Lbp^3+ 2HCS2(5)(LB^2*T)/Lbp^3;
HC(6)= HCP(6)(LB/Lbp)^4 + 2HCS(6)(LB^3*T)/Lbp^4+ 2HCS2(6)(LB^3*T)/Lbp^4;
HC(7)= HCP(7)(LB/Lbp)^4 + 2HCS(7)(LB^3*T)/Lbp^4+ 2HCS2(7)(LB^3*T)/Lbp^4;
HC(8)= HCP(8)(LB/Lbp)^5 + 2HCS(8)(LB^4*T)/Lbp^5+ 2HCS2(8)(LB^4*T)/Lbp^5;

%-------Port and Stbd HCs-----------------------------------
```

Yvhc = 2*HC(1)

Yrhc = 2*HC(2)

Nvhc = 2*HC(3)

Nrhc = 2*HC(4)

Yvdothc = 2*HC(5)

Yrdothc = 2*HC(6)

Nvdothc = 2*HC(7)

Nrdothc = 2*HC(8)

LIST OF REFERENCES

1. SLICE: A Revolutionary New Ship, Lockheed Martin Government Electronic Systems, by Terrence W. Schmidt, November 1998.

2. Principles of Naval Architecture, John P. Comstock editor, Society of Naval Architects and Marine Engineers, 1967.

3. Principles of Naval Architecture, v III, Edward V. Lewis editor, Society of Naval Architects and Marine Engineers, 1989.

4. Papoulias, Fotis A. *Informal lecture notes for Marine Vehicle Dynamics ME 4823*, Naval Postgraduate School, CA, 1993.

5. Healey, A. *Informal lecture notes for Marine Vehicle Dynamics ME 4823*, Naval Postgraduate School, CA, 1993.

6. Naval Coastal Systems Laboratory, Prediction of Acceleration Hydrodynamic Coefficients for Underwater Vehicles from Geometric Parameters, NCSL-TR-327-78, by D.E. Humphreys and K. Watkinson, February 1978.

7. Naval Coastal Systems Laboratory, *Methods For Predicting Submersible Hydrodynamics Characteristics*, NCSC TM-238-78, by John E. Fidler and Charles A. Smith, July 1978.

8. David Taylor Research Center, *Comparison of Full Scale and Rigid Vinyl Model Structural Responses For A Small Waterplane Area Twin Hull Craft (SSP KAIMALINO)*, by William H. Hay, August 1981.

9. Naval Surface Weapons Center, *Estimated Hydrodynamic Coefficients For A High Performance Vehicle*, by C.W. Smith, April 1976.

10. Wolkerstorfer, W. J. [1995] *A linear maneuvering model for simulation of Slice hulls*. Master's Thesis, Naval Postgraduate School, Monterey, CA.

THIS PAGE INTENTIONALLY LEFT BLANK

INITIAL DISTRIBUTION LIST

1. Defense Technical Information Center
   Ft. Belvoir, VA 22060-6218

2. Dudley Knox Library
   Naval Postgraduate School
   Monterey, California

3. Department of Mechanical Engineering Chairman, Code ME
   Naval Postgraduate School
   Monterey, CA 93943-5000

4. Engineering and Technology Curricular Office, Code 34
   Naval Postgraduate School
   Monterey, CA 93943-5000

5. Professor Fotis A. Papoulias, Code ME/PA
   Naval Postgraduate School
   Monterey, CA 93943-5000

6. LT Garrett D. Jones
   Naval Postgraduate School
   Monterey, CA 93943-5000